DOI: 10.1534/genetics.106.065011

Genetic Modifiers of the Drosophila *Blue Cheese* Gene Link Defects in Lysosomal Transport With Decreased Life Span and Altered Ubiquitinated-Protein Profiles

Anne Simonsen,*,† Robert C. Cumming,* Karine Lindmo,† Vanessa Galaviz,* Susan Cheng,* Tor Erik Rusten† and Kim D. Finley*,[1]

**Cellular Neurobiology Laboratory, The Salk Institute for Biological Studies, La Jolla, California 92037 and* †*Department of Biochemistry, Center for Cancer Biomedicine, The Norwegian Radium Hospital, Montebello, 0310 Oslo, Norway*

Manuscript received February 22, 2007
Accepted for publication April 11, 2007

ABSTRACT

Defects in lysosomal trafficking pathways lead to decreased cell viability and are associated with progressive disorders in humans. Previously we have found that loss-of-function (LOF) mutations in the Drosophila gene *blue cheese* (*bchs*) lead to reduced adult life span, increased neuronal death, and widespread CNS degeneration that is associated with the formation of ubiquitinated-protein aggregates. To identify potential genes that participate in the *bchs* functional pathway, we conducted a genetic modifier screen based on alterations of an eye phenotype that arises from high-level overexpression of Bchs. We found that mutations in select autophagic and endocytic trafficking genes, defects in cytoskeletal and motor proteins, as well as mutations in the SUMO and ubiquitin signaling pathways behave as modifiers of the Bchs gain-of-function (GOF) eye phenotype. Individual mutant alleles that produced viable adults were further examined for *bchs*-like phenotypes. Mutations in several lysosomal trafficking genes resulted in significantly decreased adult life spans and several mutants showed changes in ubiquitinated protein profiles as young adults. This work represents a novel approach to examine the role that lysosomal transport and function have on adult viability. The genes characterized in this study have direct human homologs, suggesting that similar defects in lysosomal transport may play a role in human health and age-related processes.

LYSOSOMES are critical organelles for the turnover or degradation of a wide variety of cellular constituents (Dell'Angelica *et al.* 2000). A complex series of targeting and import pathways direct the flow of material to the lysosome and defects in these pathways are associated with many progressive conditions including lysosomal storage disorders, reduced viability, and neural degeneration (Cataldo *et al.* 1996; Dell'Angelica *et al.* 2000; Brunk and Terman 2002; Cuervo 2004). There are three main vesicle-based pathways for transport of material to the lysosome: transport from the *trans*-Golgi network (TGN), the endocytotic pathway, and macroautophagy (here after called autophagy) (Shih *et al.* 2002; Klionsky *et al.* 2003; Raiborg *et al.* 2003; Luzio *et al.* 2005). Autophagy involves the sequestration of cytoplasmic material and entire organelles into double-membrane vesicles called autophagosomes, which are transported along microtubules for fusion with lysosomes, generating autolysosomes where the sequestered material is degraded (Klionsky and Emr 2000). Groundbreaking genetic studies in yeast have allowed the identification and characterization of nearly 30 conserved autophagy (*atg*) genes (Klionsky *et al.* 2003). Inactivation of key components within the pathway has revealed that autophagy primarily functions as an adaptive response to starvation or cellular stress by recycling nonessential cellular components for nutrition or by clearing old or damaged cytoplasmic material and organelles (Scott *et al.* 2004; Komatsu *et al.* 2005). Recent genetic studies in mice have shown that ablation of the *atg5* and *atg7* genes in the CNS leads to progressive neurological defects, the formation of ubiquitinated inclusion bodies or protein aggregates, and neuronal cell death (Hara *et al.* 2006; Komatsu *et al.* 2006).

Previously we have shown that mutations in the Drosophila *blue cheese* (*bchs*) gene result in a reduced adult life span and age-related neuronal degeneration. These defects include neural atrophy and cell death, preceded by the accumulation of ubiquitin-conjugated protein aggregates throughout the adult CNS (Finley *et al.* 2003). Consistent with these findings is the recent characterization of *Alfy* (autophagy-linked FYVE protein) the conserved human *bchs* homolog (Figure 1a) (Simonsen *et al.* 2004). Under starvation conditions or following proteasome inhibitor treatment Alfy relocalizes

[1]*Corresponding author:* Cellular Neurobiology Laboratory, The Salk Institute for Biological Studies, 10010 North Torrey Pines Rd., La Jolla, California 92037. E-mail: finley@salk.edu

from the nuclear membrane to cytoplasmic structures containing ubiquitin and early autophagic markers (Simonsen *et al.* 2004). Both Bchs and Alfy proteins are very large, highly conserved proteins that are nearly 400 kDa in size (~50% identity between fly and human homologs) (Finley *et al.* 2003; Simonsen *et al.* 2004). Both proteins contain several conserved protein domains in the C terminus: a BEACH domain followed by a series of WD40 repeats and a PI(3)P-binding FYVE domain (Figure 1a) (Finley *et al.* 2003; Simonsen *et al.* 2004). The N-terminal two-thirds of Bchs/Alfy (>2000 amino acids) are also conserved, but do not contain readily identifiable functional domains. However, this region is leucine/isoleucine rich and modeling programs suggest the presence of leucine zippers and coiled-coil domains. On the basis of this sequence analysis it is likely that Bchs/Alfy serve as scaffolding proteins, mediating a diverse series of protein and lipid interactions promoting the recruitment, organization, and transport of vesicles. Taken together, this information suggests that the Bcsh/Alfy family aids in the removal of cytoplasmic ubiquitinated protein aggregates by promoting their autophagic clearance (Bjorkoy *et al.* 2005). This protein family is not found in yeast and the Bchs/Alfy proteins may have a greater role in multicellular organisms in protein clearance than in starvation-induced autophagy (Finley *et al.* 2003; Simonsen *et al.* 2004). However, the cellular pathway(s) that Bchs participates in remains poorly understood.

A recent study showed that overexpression of Bchs in the eye using a *GMR-Gal4* driver results in a rough eye phenotype (Khodosh *et al.* 2006). Using a genetic modifier screen, 195 chromosomal deficiency lines were crossed to the Bchs overexpressing line and individual genes uncovered by a single deletion (93B6–7; 93D2) were examined further for Bchs interaction (Khodosh *et al.* 2006). Individual *rab11* mutations were found to significantly enhance the dominant Bchs eye phenotype and additional studies revealed that the Rab11 and Bchs proteins colocalize at the neuromuscular junction and affect bristle development and synaptic function (Khodosh *et al.* 2006). In this report, we show that overexpressing Bchs in the eye (*GMR-Gal4* driver) also results in a rough eye phenotype that is accompanied by the formation of ubiquitin containing varicosities along photoreceptor neural projections. This phenotype is also seen when Bchs is overexpressed in larval motor neurons and is similar to defects associated with perturbations of vesicle transport or fusion pathways (Torroja *et al.* 1999; Gunawardena and Goldstein 2001; Kraut *et al.* 2001; Nixon *et al.* 2005). We further show that young *bchs* mutants and flies overexpressing Bchs display an altered accumulation profile of ubiquitinated (UB) proteins. Collectively, these findings suggest that Bchs affects protein and vesicle trafficking and is consistent with its role in the transport of lysosomal substrates. To further investigate potential *bchs* genetic interactions an extensive genetic screen based on alteration of the Bchs eye phenotype was used to identify several unique modifier loci (FlyBase 2007). From this study recessive mutations in lysosomal trafficking genes and cytoskeletal and motor proteins as well as in members of the ubiquitin and SUMO signaling pathways were found to have potential genetic interactions with Bchs (FlyBase 2007). To further characterize mutant phenotypes, mutations in lysosomal genes that produced viable adult flies were examined for UB-protein profiles and changes to adult longevity. As with *bchs* mutants, the functional losses of several lysosomal transport genes also alter high-molecular-weight UB-protein profiles and reduce adult longevity. Together the genetic analyses of several lysosomal trafficking genes provide a novel mechanistic insight into the requirement of these pathways for the long-term viability of adult Drosophila.

MATERIALS AND METHODS

Protein sequence analysis and motifs: Identification and characterization of potential functional domains encoded within the Bchs and Alfy protein sequences were performed using online modeling algorithms including http://scansite.mit.edu/motifsca and http://www.ncbi.nlm.nih.gov/Structure/.

Fly culture and stocks: Flies were cultured and maintained on standard cornmeal–molasses–yeast-based medium. The transgenic line, *EP(2L)2299* was originally from the Rörth collection of *P*-element insertions and allows Gal4-driven expression of the full-length Bchs protein (Rorth 1996; Kraut *et al.* 2001). The $bcsh^{5}$ allele and revertant lines that were derived from excision of the *EP(2L)2299 P* element have been described previously and are outlined in Figure 1b (Finley *et al.* 2003). The *bchs P*-element insertion allele, $bcsh^{3}$ was maintained as a stock over the *Df(2L)clot7* chromosome [*402-11Cy/Df(2L)clot7*] and used for aging and starvation studies (Finley *et al.* 2003; FlyBase 2007). Drosophila stocks screened in this study were primarily obtained from the Bloomington Stock Center (stock numbers are noted in Figure 2 and Table 1) (FlyBase 2007). The $hook^{11}$ allele was a gift from H. Kramer (University of Texas Southwestern) (Kramer and Phistry 1999) and the *UAS-GFP-CAAX* (membrane-targeted GFP) and *GMR-Gal4* transgenic lines have been described previously (Finley *et al.* 1998).

Western analysis of the Bchs protein and ubiquitinated conjugated proteins: Groups of 50 fly heads per genotype were collected and homogenized in 1× PBS, 0.1% Triton-X buffer containing protease inhibitors (4°). After centrifugation the supernatants were collected for each genotype and saved as the protein concentrations were determined for each sample using a Lowry assay (Bio-Rad, Hercules, CA). Twenty micrograms of total protein for each sample were loaded and resolved on 4–20% gradient gels (Bio-Rad) and electroblotted. Western blots were probed sequentially with anti-Bchs (1:4000 dilution, polyclonal rabbit, a gift from Kia Zinn, Division of Biology, California Institute of Technology, Pasadena, CA) or anti-Actin antibodies (1:200 dilution, mouse monoclonal JLA20, developed by Jim Jung-Ching Lin and obtained from the Developmental Studies Hybridoma Bank developed under the auspices of the National Institute of Child Health and Human Development and maintained by The University of Iowa, Department of Biological Sciences, Iowa City, IA). For

Western analysis of ubiquitinated proteins, 6 heads for each genotype (1-day-old flies) were collected and sonicated in 100 μl protein lysis buffer (2% SDS) and centrifuged. Twenty-five microliters of each sample were run on a 4–20% gradient gel and Western blots were probed sequentially with anti-Ubiquitin (1:1000 dilution, Cell Signaling), anti-Actin, and anti-Bchs antibodies. Following hybridization with appropriate secondary antibodies, immunoreactive bands were detected using standard enhanced chemiluminescence reagents. Autoradiographs were digitally scanned using a GS-800 calibrated desitometer and ImageQuant imaging software and the relative amount of Bchs protein for a given genotype was corrected using actin as a loading control.

Fluorescence confocal microscopy: Staged third instar larvae and pupae from the *UAS-GFP-CAAX,GMR-Gal4* stock line or from the *UAS-GFP-CAAX,GMR-Gal4/EP(2)2299* cross were dissected, fixed in 3.5% paraformaldehyde and PBS, and rinsed in PBT (0.05% Triton-X). Tissues were mounted and assayed directly for GFP expression patterns or used for costaining with anti-Bchs or anti-ubiquitin antibodies. For costaining, tissues were fixed in 3.5% paraformaldehyde and PBS for 1 hr at 4° and washed three times in PBT (0.05% Triton-X) at 4°. Following three washes in PBT, tissues were incubated in 5% normal goat serum, PBT, and anti-Bchs (1:1000 dilution; Kia Zinn, Caltech) or with anti-ubiquitin antibodies (1:200 dilution, mouse monoclonal; Cell Signaling) for 2 hr at room temperature, washed three times, and then incubated for 1 hr at room temperature with Cy3-conjugated anti-rabbit or anti-mouse secondary antibodies (1:200 dilution; Jackson Laboratories). Tissues were washed three times in PBT and mounted. Images were collected using a Leica TCS SP2 AOBS confocal microscope.

Design of the Bchs gain-of-function modifier screen: A Bchs-based gain-of-function (GOF) screen was made possible by a characterization fly line containing an EP-UAS modular expression transposable element insertion, *EP(2L)2299*, which is located upstream of the *bchs* coding sequence (Rorth 1996). Previous work reported that this UAS-*P* element allowed overexpression of full-length Bchs protein in motor neurons and generated a dominant GOF phenotype (Kraut *et al.* 2001). Overexpressing Bchs in the eye using the *GMR-Gal4* driver also produces a highly reproducible dominant phenotype. The GOF phenotype is sensitive to Bchs dosage as shown in flies containing an additional copy of *EP(2L)2299* or two copies of both transgenes (Figure 2a). The *GMR-Gal4* and *EP(2L)2299 P* elements were recombined onto a single chromosome and kept as a heterozygous stock by placing it over a double second and third chromosome balancer (*CyO:TM6B, Tb1*) (FlyBase 2007). Most lines selected for testing in this screen were obtained from the Bloomington Stock Center. Initially we examined stocks representing the majority of the second and third chromosome Bloomington deficiency kits. Subsequent crosses with the *GMR-Gal4,EP(2L)2299/CyO:TM6B* stock involved lines containing mutations in genes with a wide range of cellular functions. Subsequent mutations were selected that further focused the screen and represented genes involved with lysosomal transport pathways, cytoskeleton or motor proteins, or members of the ubiquitin/SUMO pathways (FlyBase 2007). Individual lines were crossed to the *GMR-Gal4,EP(2L)2299/CyO:TM6B* stock and grown at 22° and the F_1 progeny were scored for modification of eye pigmentation, size, shape, surface texture, and necrosis. On average a size decrease of 30–35% or an increase of 15–20% was set as a lower and an upper significance limit and used to classify a mutation as an enhancer or a suppressor. Representative digital eye images were taken using a Leica MZ6 dissection microscope and Nikon Coolpix 990 camera system. Images were processed and illustrations made using Adobe Photoshop 7.0 and Canvas 8.0 imaging software.

Life span analysis: Before analyzing mutant lines for changes in adult life span, each stock was first outcrossed into a Canton-S or w^{1118} background for several generations before reestablishing individual homozygous lines. During the outcrossing process individual mutant lines were assayed for life span and multiple experiments were pooled. For aging analysis at least 100 newly emerged male flies were collected for a given genotype and kept on standard Drosophila culture media (25 per vile) (Finley *et al.* 2003). Flies were placed at 25° or 29° with a 12-hr light–dark cycle and turned onto fresh food every 2–3 days, and the number of dead flies was counted. The percentage of flies remaining alive for a given time point was calculated from the total starting number of flies aged for a particular genotype. The mean genotype life span and standard deviation were determined using Microsoft Excel and the *P*-values were determined using GraphPad online software (http://www.graphpad.com).

RESULTS

Characterization of the *bchs EP(2L)2299 P* element and Bchs expression profiles: While *bchs*'s loss-of-function (LOF) phenotypes make it an interesting model to study progressive neural degeneration, the subtlety and timing of its adult defects has prevented the efficient design of genetic screens to clarify *bchs*'s functional pathway or to identify potential interacting partners (Finley *et al.* 2003). We therefore characterized a *P*-element insertion located in *bchs* [*EP(2L)2299*] that could be used to design a dominant GOF genetic modifier screen. Previously we had mapped and sequenced the entire genomic region and cDNA sequence of the *bchs* gene and carried out a *P*-element mutagenesis screen on the basis of excision of the *EP(2L)2299* construct (Figure 1b). Molecular analysis showed that the *EP(2L)2299 P*-element line contains a single insertion located within the first *bchs* intron, upstream of the *bchs* open reading frame (Figure 1b). Using genetic crosses with a stock containing a constitutively active transposase (Δ2-3), the *EP(2L)2299 P* element was excised and individual flies lacking the *white*+ marker were used to generate stocks and characterized for both precise and imprecise removal of the *P* element. Both types of excisions were identified and characterized for *bchs* expression and mutant phenotypes (Finley *et al.* 2003; Simonsen *et al.* 2004). The $bchs^{5}$ allele (Ex22) represents an imprecise excision that removes most of the first and second introns and the second and third exons, effectively eliminating the start codon of the message (Figure 1b). Other lines representing precise excisions were identified that restore the original *bchs* sequence and gene structure (Figure 1b, $bchs^{rev1}$). Western analysis of proteins made from 1-day-old adult heads revealed that the $bchs^{5}$ mutation eliminates the production of Bchs, while the $bchs^{rev1}$ line has normal levels of the protein (Figure 1c, samples 1 and 2). Young *EP(2L)2299* flies display a

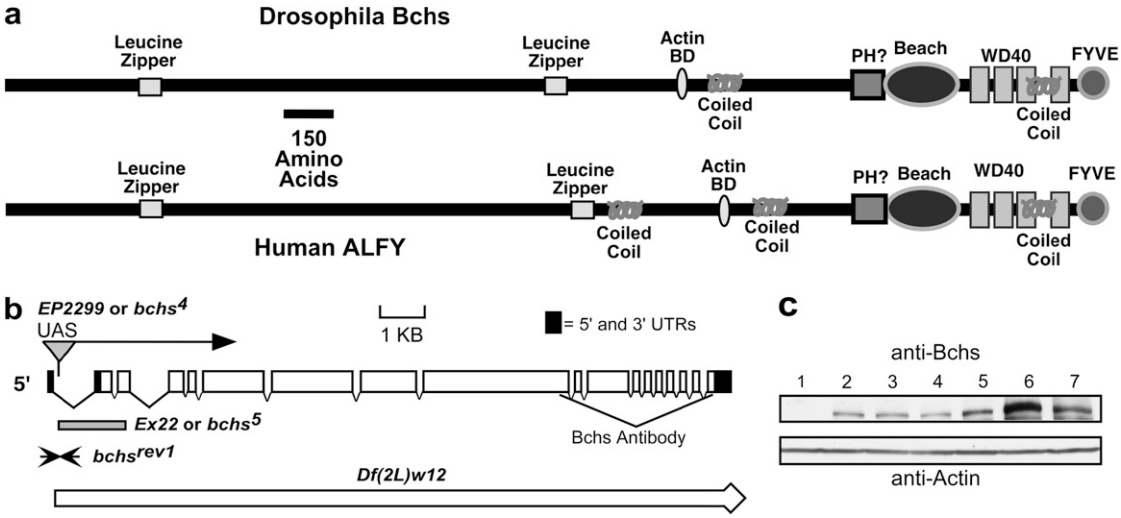

FIGURE 1.—Functional motifs of Bchs/Alfy, mutant alleles, and protein profiles. (a) Members of the *bchs/Alfy* gene family encode very large, highly conserved proteins with several potential functional protein domains. The C terminus contains a FYVE finger motif [binds PtdIns(3)P lipids], a BEACH domain, and a series of WD40 repeats (protein–protein interaction domain). The remaining N-terminal ~2000 amino acids of the Bchs and Alfy proteins are also highly conserved and leucine–isoleucine rich. Motif-modeling programs predict several leucine-based motifs including leucine zippers and coiled-coil domains, which primarily facilitate protein interactions and dimerization. Further sequence analysis identifies a second potential phosphatidylinositol interaction motif (PH domain). Sequence analysis of the Bchs/Alfy family indicates that these proteins likely facilitate a diverse series of protein interactions as well having close associations with membrane vesicles. (b) The insertion site of the *EP(2L)2299* transposable element is located in the first intron of *bchs* and allows Gal4-driven expression of the full-length Bchs protein. The Df(2L)w12 deletion was characterized during our the initial characterization and mapping of the *bchs* and *dsf* genes and removes nearly 60 kb of genomic sequence containing both genes. Several lines were also isolated that represent individual *P*-element excisions that generate microexcision alleles of *bchs* (Ex22 or $bchs^5$) or fully restore the gene ($bchs^{rev1}$). (c) Western analysis of protein extracts made from adult heads shows that Bchs is a large protein (>250 kDa) that is absent from $bchs^5$ mutants (1) and is expressed at normal levels in $bchs^{rev1}$ animals (2). Young homozygous *EP(2L)2299* flies (3) produce Bchs at levels that are similar to those of Canton-S (4) and w^{1118} (5) control animals. The Bchs protein is increased fivefold when overexpressed in *EP(2L)2299,GMR-Gal4* flies (6) above that of Canton-S flies (4). Using a small deletion that eliminates one *bchs* allele reduces the total level of Bchs even when it is overexpressed in the eye [*EP(2L)2299,GMR-Gal4/Df(2L)W12*] (7).

Bchs expression pattern similar to that of our previous findings (becomes absent in older animals) and further phenotypic characterization of this line indicated that it is as a hypomorphic or weak allele of *bchs* (Figure 1c, sample 3) (FINLEY *et al.* 2003). Crossing the *EP(2L)2299* line with *GMR-Gal4* flies (eye driver) produces F_1 offspring that have at least a fivefold increase in the total levels of Bchs within the head (Figure 1c, samples 6 and 4). However, protein levels are substantially decreased when the *EP(2L)2299,GMR-Gal4* chromosome is combined with a deletion that removes the entire *bchs* genomic region (thereby eliminating the wild-type Bchs expression) but remain elevated well above that of controls [Figure 1c, sample 7, *Df(2L)W12*] (FINLEY *et al.* 2003).

Bchs's GOF eye phenotype: We observed that overexpression of Bchs [*GMR-Gal4,EP(2L)2299*] led to a morphologically distinct external eye phenotype (Figure 2a). When compared to wild-type controls and the individual parental lines, the *GMR-Gal4,EP(2L)2299* combination results in a dark eye pigmentation (similar to *GMR-Gal4*), a roughened eye surface texture, and a slight decrease in the overall eye size. The dominant phenotype is sensitive to the dosage of Bchs as an additional copy of *EP(2L)2299* and two copies of both *GMR-Gal4* transgenes further exacerbate the eye phenotype. Excess Bchs in photoreceptor cells (normally expressed at much lower levels) also alters the neural projection patterns. These defects can be visualized by coexpressing *bchs* with a membrane-targeted GFP (*UAS-GFP-CAAX*) (FINLEY *et al.* 1998). Wild-type eye discs (third instar larvae) display the classic ommatidial organization for this point in retinal development (Figure 2b). In contrast, *GMR-Gal4,EP(2L)2299* eye discs have a slight loss in morphology and a decrease in the brightness of the central ommatidial region (Figure 2c, arrows), which marks the confluence of photoreceptor axons before exiting the eye disc.

The innervation patterns of R7 and R8 photoreceptors into the optic lobes can also be visualized in midpupal control and Bchs-overexpressing animals. Wild-type pupae demonstrate the normal stereotypic array of R7 and R8 projections, as well as normal axonal and growth cone morphology for this development stage (Figure 2b) (FINLEY *et al.* 1998; DITCH *et al.* 2005). In the Bchs-overexpressing flies the number and basic array of R7 and R8 axonal projections remain relatively normal (Figure 2c). However, there is a loss of growth cone

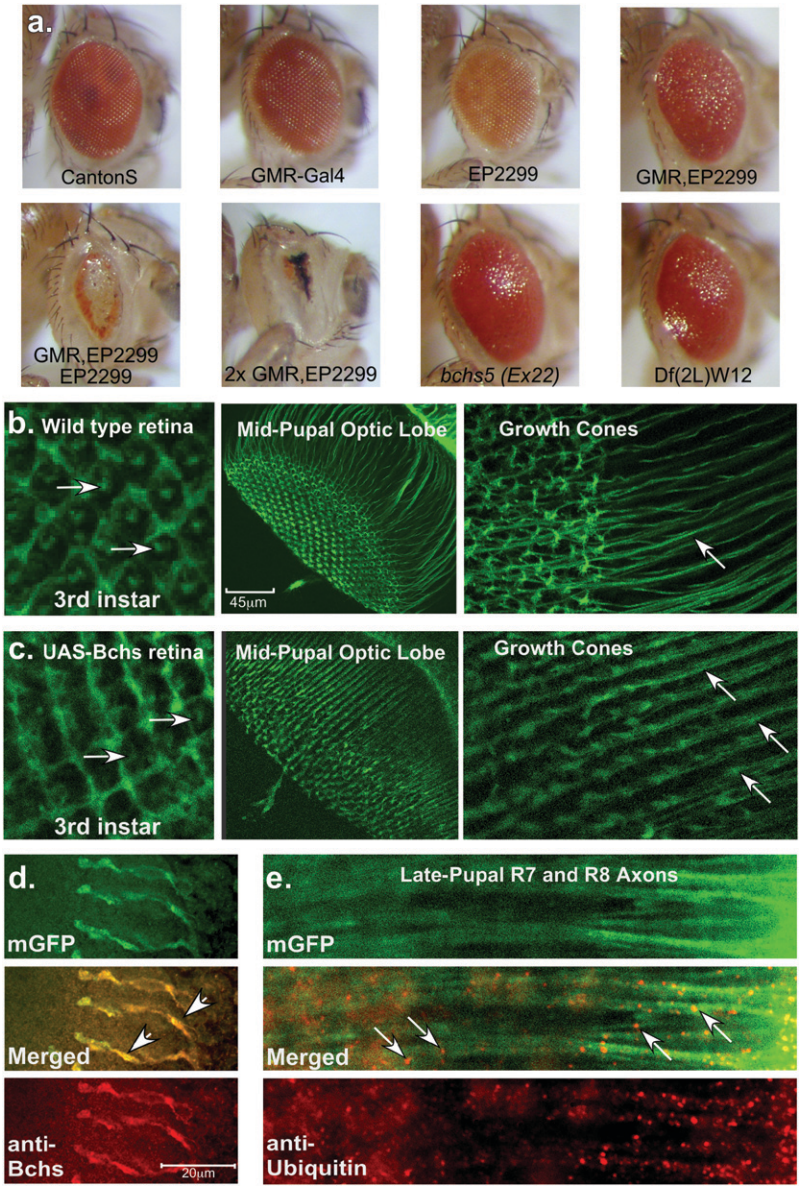

Figure 2.—Phenotypes resulting from Bchs overexpression. (a) Characteristic external eye phenotypes of wild type, *GMR-Gal4*, *EP(2L)2299*, *GMR-Gal4,EP(2L)2299*, and 2X *GMR-Gal4*, *EP(2L)2299* flies. (b) Left to right: confocal images from control flies expressing *GMR-Gal4/UAS-GFP-CAAX*, which express a membrane-targeted green fluorescent protein, show the developing retina (arrows indicate convergence of photoreceptor axons) and neural projections of R7 and R8 photoreceptors (midpupae). (c) Left to right: age-matched tissues from flies coexpressing Bchs [*EP(2L)2299*]. Retinal development is relatively normal but neural projections into the optic lobe show subtle defects in patterning and growth cone (GC) formation. Arrows indicate the formation of varicosities along the length of axons. (d) In late pupae immunostaining for Bchs shows high levels of Bchs in late pupal axons in *EP(2L)2299*-overexpressing animals. Bchs colocalizes to terminal synapses and regions of axonal swelling (arrows). (e) In late pupae, ubiquitinated protein aggregates or vesicles (arrows) can be detected along the length of photoreceptor axons in *EP(2L)2299*-overexpressing animals. These structures are not seen in age-matched wild-type controls (data not shown).

morphology as well as axonal swelling or varicosities. At higher magnification, control flies show normal axonal projection patterns (Figure 2b, arrow) and growth cone (GC) morphology, while Bchs overexpression results in the loss of growth cone definition and premature termination of developing synapses. These axons also show the formation of varicosities (Figure 2c, arrows). The R7 and R8 terminal synapses are also abnormal and the Bchs protein can be detected near areas of axonal distension (Figure 2d, arrows). These findings are similar to those of previous studies showing that excess Bchs results in synaptic defects and the formation of axonal bulges both in larval motor neurons (Kraut *et al.* 2001) and in photoreceptors (Khodosh *et al.* 2006).

Increased Bchs expression in neural projections results in the formation of varicosities containing ubiquitin-immunopositive inclusions or vesicles (Figure 2e, arrows), which are not detected in wild-type axons (data not shown). Flies with mutations in the *bchs* gene display a similar phenotype in which ubiquitinated protein profiles are altered in adult neural tissues (Finley *et al.* 2003; Simonsen *et al.* 2004). This suggests that either a decrease or overproduction of Bchs can result in the altered accumulation of UB proteins. To quantitatively examine this, Western analysis was performed on protein extracts prepared from heads taken from 1-day-old control flies (Canton-S), homozygous $bchs^4$ mutants [*EP(2)2299*], and *bchs*-overexpressing animals [*GMR-Gal4,EP(2)2299*] as well as from flies expressing the *dissatisfaction* (*dsf*) gene (*GMR-Gal4/UAS-dsf*) (Figure 3a) (Pitman *et al.* 2002). Although it is a remote possibility the *EP(2)2299 P* element could potentially increase the expression of a gene located distal to *bchs*. Therefore Dsf-overexpressing flies (*GMR-Gal4/UAS-dsf*) were selected as a control since the endogenous *dsf* gene is located distal to *bchs* and is the only other gene in the

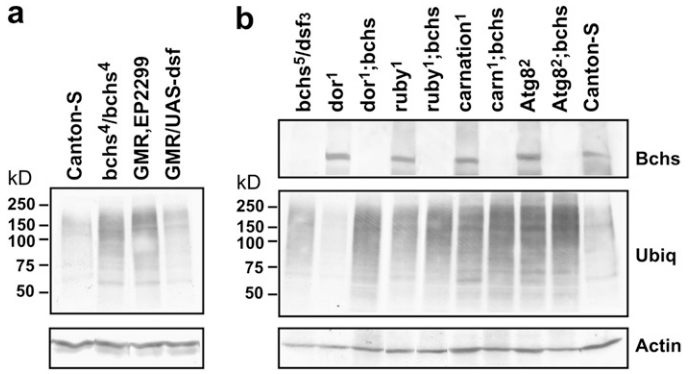

FIGURE 3.—Ubiquitinated protein profiles. The heads from young adult flies were collected and the ubiquitinated protein profiles (UB proteins) were examined by Western blot analysis. (a) Wild-type flies (Canton-S) show low levels of UB proteins while homozygous *bchs*^{4} mutants [*EP(2)2299*] and flies overexpressing Bchs [*GMR-Gal4,EP(2)2299*] show enhanced accumulation of high-molecular-weight UB proteins. Flies overexpressing *dsf* (*GMR-Gal4/UAS-dsf*), a gene downstream of *bchs*, do not show an increase in UB proteins. (b) Flies containing the *deep orange*^{1}, *ruby*^{1}, *carnation*^{1}, and *Atg8a*^{2} mutations were crossed into the *bchs*^{5}*/Df(2L)dsf3* genetic background. Head homogenates from young male flies were Western blotted and sequentially probed for ubiquitin, actin, and Bchs. Again, *bchs* mutant animals (*bchs*^{5}*/dsf3*) show an early accumulation of UB proteins, as do flies containing single mutations in the *ruby*^{1}, *carnation*^{1}, and *Atg8a*^{2} genes. Several genotypes with mutations in two lysosomal transport genes saw a synergistic enhancement in UB-protein levels. They include *dor*^{1}*;bchs*^{5}*/dsf3*, *ruby*^{1}*;bchs*^{5}*/dsf3*, *carnation*^{1}*;bchs*^{5}*/dsf3*, and *Atg8a*^{2}*;bchs*^{5}*/dsf3* mutant combinations. (c) Densitometry values were used to normalize UB proteins against actin levels as loading controls and compared with the corrected Canton-S levels to calculate the fold increase in UB proteins. Flies with the *dor*^{1}*;bchs*^{5}*/dsf3* and *carnation*^{1}*;bchs*^{5}*/dsf3* genotypes had the most pronounced synergistic increase while *ruby*^{1}*;bchs*^{5}*/dsf3* and *Atg8a*^{2}*;bchs*^{5}*/dsf3* flies show a minor enhancement. In the case of the *Atg8a*^{2}*;bchs*^{5}*/dsf3* genotype this may be due to the extreme elevation in UB-protein levels seen in *Atg8a*^{2} single-mutant flies.

correct orientation for activation by the *EP(2)2299 P* element. In young *EP(2)2299* flies UB proteins are elevated when compared to controls, which is consistent with our previous results showing that loss of *bchs* alters protein profiles (FINLEY *et al.* 2003). In flies overexpressing *bchs* [*GMR-Gal4,EP(2)2299*] a significant increase is also seen in the accumulation of high-molecular-weight UB proteins. In contrast, driving *dsf* expression in the eye (*GMR-Gal4,UAS-dsf*) does not alter UB-protein levels (Figure 3a) (PITMAN *et al.* 2002). This demonstrates that functional loss and overproduction of *bchs* both result in the accumulation of UB proteins in neural tissues. In addition, these data show that while activation of the *UAS-dsf* transgene produces extensive defects in eye development, these defects are distinct from those produced by excess Bchs (PITMAN *et al.* 2002). These data indicate that transcriptional activation by the *EP(2)2299* UAS-*P* element results in an increase only in *bchs* expression and produces a gene-specific eye phenotype.

The easy to score dominant eye phenotype from Bchs overexpression provided an opportunity to develop an effective modifier screen. Dominant modifier screens using overexpression of a specific protein have been employed to characterize several diverse genetic pathways including those associated with RAS/MAPK signaling (*i.e.*, *GMR-yan*^{act} or *Sev-yan*^{act}) as well as Armadillo and Notch functions (VERHEYEN *et al.* 1996; GREAVES *et al.* 1999; REBAY *et al.* 2000). These types of modifier screens have been used successfully to identify factors that alter polyglutamine aggregation and mutant τ-toxicity (FERNANDEZ-FUNEZ *et al.* 2000; KAZEMI-ESFARJANI and BENZER 2000; SHULMAN and FEANY 2003). In the case of Bchs, excessive levels of the protein may deplete interacting cofactors, resulting in the formation of incomplete protein complexes that block axonal transport or prevent the formation or targeting of vesicle subtypes. Eye phenotypes similar to Bchs are observed when SNAP1 (a protein involved with vesicle fusion) is expressed using the same *GMR-Gal4* driver (BABCOCK *et al.* 2004). *UAS-SNAP1* expression in motor neurons disrupts the formation of neuromuscular junctions and in the eye produces a mild rough eye phenotype that is further exacerbated with higher levels of the protein (BABCOCK *et al.* 2004). Furthermore, *UAS-SNAP1* expressed in combination with mutant alleles of interacting partners (*dNSF2*^{155} and *syx*$^{\Delta 229}$) enhances the eye phenotype (including changes to pigmentation, surface texture, and the overall size of the eye), while coexpression of wild-type *UAS-dNSF1* or *UAS-NSF2* suppresses these defects (BABCOCK *et al.* 2004). Therefore we used overexpression of Bchs in the eye to design of a GOF screen. Similar to the previous study by KHODOSH *et al.* (2006) we initially examined a set of chromosomal deletion lines but then primarily focused on individual recessive loss-of-function mutations in a wide range of genes involved with protein turnover, vesicle trafficking, or lysosomal development or function.

Bchs GOF modifier screen: The similarity between the *EP(2L)2299* and the *UAS-SNAP1* overexpression eye phenotypes indicated that a modifier screen could be used to detect Bchs interactions using a dominant GOF eye phenotype. For this screen the *GMR-Gal4,EP(2L)2299/CyO:TM6B* stock line was established and used for individual crosses to mutant lines. Due to the use of the GAL4/UAS system to produce elevated levels of a very large protein (with potentially complex interactions) we were concerned that coexpressing additional proteins

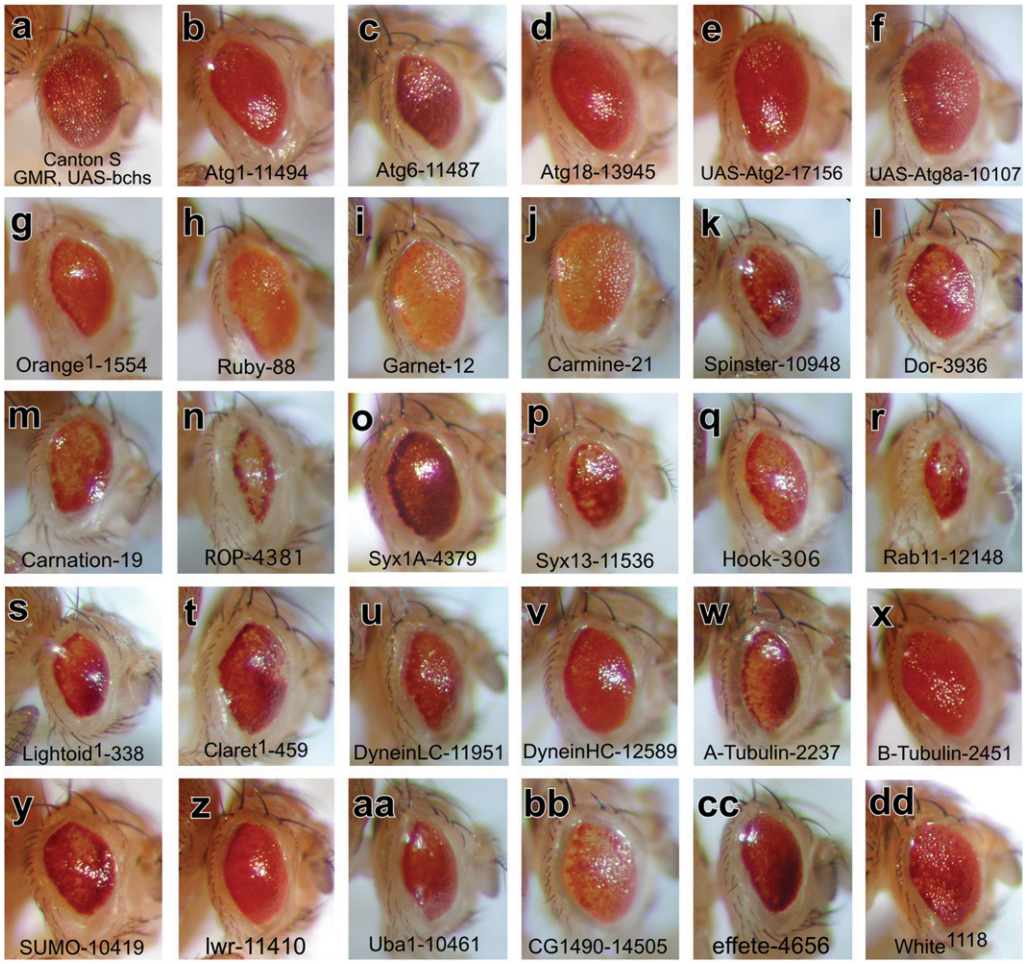

FIGURE 4.—Bchs eye modifiers: fly eyes representing one copy of the *GMR-Gal4,EP(2L)2299* expression transgenes in (a) wild-type control (Canton-S) or in heterozygous mutant backgrounds. Mutations in autophagy genes (b) *atg1* and (c) *atg6* enhance the eye phenotype while (d) a *P*-element mutation in *atg18* has only a slight effect on the Bcsh-GOF phenotype. Coexpression of (e) *UAS-atg2* and (f) *UAS-atg8a* was scored as phenotype suppressors. Mutations in (g) *orange* (*or*, adaptor complex AP-3 ξ-subunit) act as phenotype enhancers, while mutations in (h) *ruby* (*rb*, AP-3 β-subunit), (i) *garnet* (*g*, AP-3 δ-subunit), and (j) *carmine* (*cm*, AP-3 μ-subunit) are complex modifiers. Mutations in other vesicle-trafficking genes including (k) *spinster* (*spin*), (l) *deep orange* (*dor*), (m) *carnation* (*car*), (n) *ras opposite* (*rop*), (o) *syntaxin1A* (*syx1A*), (p) *syntaxin13* (*syn13*), (q) *hook (hk)*, (r) *rab-protein 11* (*Rab11*), (s) *lightoid* (*ltd*), and (t) *claret* (*ca*) all act as strong Bchs-GOF enhancers. Other proteins involved in lysosomal transport are also Bchs enhancers and include mutations in the (u) *dyneinLC* and (w) α-*tubulin* genes and to a much lesser extent (v) *dyneinHC* and (x) β-*tubulin* mutations. Mutations in SUMO and ubiquitin pathway members are Bchs-GOF enhancers and include (y) *SUMO*, (z) *lesswright* (*lwr*), (aa) *Uba1*, (bb) *C-terminal ubiquitin hydrolase* (CG1490), and (cc) *effete* mutations. (dd) The *GMR-Gal4,EP(2L)2299* transgenes in a *white*^{1118} background are shown as a nonmodifying negative control.

could lead to a large number of false positives. Therefore, we primarily examined lines that represented recessive loss-of-function mutations and focused on identifying genetic interactions that enhanced the eye phenotype. This design had the advantage of allowing lethal deletions or mutants to be examined. The *GMR-Gal4,EP(2L)2299* stock was initially crossed to lines from the second and third chromosome deficiency kits (Bloomington Stock Center). These results are included in supplemental Tables 1 and 2 at http://www.genetics.org/supplemental/. Most lines do not significantly alter the eye phenotype and those lines that do behaved as enhancers. This initial screen implied that a wide range of genes did not behave as significant modifiers of the *GMR-Gal4,EP(2L)2299* phenotype.

Additional lines were screened that represent recessive loss-of-function mutations in specific genes. Initially, mutant lines were selected if their genomic location overlapped with deletion chromosomes that behaved as modifiers. Subsequent lines were chosen that represented divergent cellular pathways affecting lysosomal/endosomal trafficking, neural function or development, synaptic vesicle transport or fusion, and adult life span and cellular metabolism. Later, several UAS lines that affected autophagy gene expression were also included. In all cases F_1 progeny were scored for changes in adult eye size, shape, pigmentation, and surface texture. Again, most genetic combinations with *GMR-Gal4,EP(2L)2299* did not significantly modify the eye phenotype, indicating a degree of specificity in the detection of potential *bchs* genetic interactions. These results are outlined in supplemental Table 3 at http://www.genetics.org/supplemental/. Examples of genetic mutations that did behave as modifiers of the Bchs GOF phenotype are illustrated in Figure 4 and are further detailed in Table 1 (individual lines and mutation type). To control for phenotypes resulting from dominant or nonspecific interactions with the *GMR-Gal4* driver, lines that were scored as modifiers were crossed individually to the *GMR-Gal4* driver and the F_1 offspring were

TABLE 1

Enhancers and suppressors of Bchs overexpression eye phenotype

Gene and allele	Modification	Bloomington stock no.	Homologs, protein domains, and functions
		Vesicle trafficking	
atg1^{00305}	En	11484	Serine/threonine kinase, Tor effector
atg6^{00096}	En	11487	Beclin-1, mitochondrial protein
atg18^{KG03090}	WEn	13945	WD40 domains, binds PIP3-5P2 lipid
atg2^{EP3697}	Su	17156	Hydrophilic protein, preautophagic structure
atg8a^{EP362}	Su	14639	LC3, lipid attachment and microtubule binding
orange^{49h}	En	2385	ξ-subunit of AP-3 complex
ruby^{1}	En/Su	88	β-subunit of AP-3 complex
garnet^{1}	En/Su	12	δ-subunit of AP-3 complex
carmine^{1}	En/Su	21	μ-subunit of AP-3 complex
spinster^{k09905}	En	10948	Integral membrane protein
deep orange^{1}	En	3936	Vps18p, ubiquitin ligase E3
deep orange^{4}	En	35	Vps18p, ubiquitin ligase E3
deep orange^{8}	En	28	Vps18p, ubiquitin ligase E3
carnation^{1}	En	19	Vps 33, sec1 protein
ras opposite^{G27}	SEn	4381	Rop, munc-18, n-Sec1
syntaxin 1A$^{\Delta 229}$	En	4379	SNARE, coiled-coil, vesicle targeting
syntaxin 13^{01470}	En	11536	SNARE, coiled-coil, vesicle targeting
hook^{1}	En	306	Coiled-coiled, MVB interactions
rab11^{93Bi}	SEn	4158	Small GTPase
rab11^{j2D1}	SEn	12148	Small GTPase
lightoid^{1}	En	338	Rab-RP1, a GTPase
claret^{1}	En	459	Guanine nucleotide exchange factor (GEF)
		Cytoskeletal and motor proteins	
dlic2^{G0190}	En	11951	Dynein LC, microtubule-based motor activity
dlic2^{G0065}	En	11696	Dynein LC, microtubule-based motor activity
btv^{BG01771}	En	12589	Dynein HC, microtubule-based motor activity
α-*tubulin84B*^{5}	En	2412	84B, cytoskeletal and microtubule constituent
α-*tubulin84B*^{7}	En	2237	84B, cytoskeletal and microtubule constituent
β-*tubulin* ^{D}	WEn	2451	85D, cytoskeletal and microtubule constituent
		Ubiquitin and SUMO pathway	
smt3^{k06307}	En	10419	SUMO, ubiquitin-like protein
lesswright^{r05486}	En	11410	SUMO-conjugating enzyme
uba1^{s3484}	En	10461	E1 ubiquitin-activating enzyme
effete^{mer1}	En	4656	UbcD1, ubiquitin-conjugating enzyme
CG1490	En	14505	Ubiquitin-specific protease 7

Modifier genes that also demonstrate a phenotypic change with a corresponding deletion chromosome from the second and third deficiency kit screens are underlined. En, enhancer; WEn, weak enhancer; Su, suppressor; En/Su, complex modifier; SEn, strong enhancer.

independently examined for eye morphology changes. Individual modifier genes that also demonstrated a phenotypic change with a corresponding deletion chromosome from the second and third chromosome deficiency kit screen are noted in Table 1. Of the 20 individual second or third chromosome mutations identified as modifiers, a total of 6 showed an eye phenotype that was similar to the overlapping deletion allele. Significant changes to eye phenotypes were not observed when the *GMR-Gal4* driver was used to overexpress independently several other autophagy genes (individual EP-UAS lines) or in combination with recessive loss-of-function mutations (results are shown in supplemental Figure 1 at http://www.genetics.org/supplemental/).

Modifying autophagy genes: Of the six Drosophila autophagy genes examined in this study, mutations in *Atg1* (serine/threonine kinase) and *Atg6* (Beclin-1) were scored as moderate eye enhancers, while functional loss of the *Atg18* gene [PtdIns(3,5)P_2 binding protein] only had a minor effect (Figure 4, b–d). In contrast, coexpression of *atg2* (EP-UAS line) and *atg8a* (EP-UAS line) moderately suppressed the Bchs-GOF phenotype (Figure 4, e and f) (FlyBase 2007). Individually these autophagy mutations act as strong homozygous lethal alleles, resulting in death at the late pupal or young adult stage of life. The notable exception is an adult viable mutation in the *atg8a* gene (data not shown). Their adult survival may in part reflect a partial functional redundancy from a second *atg* gene, *atg8b* (third

chromosome) (FlyBase 2007). Atg8, also called LC3 (light chain of the microtubule-associated protein complex, MAP), undergoes C-terminal cleavage and covalent linkage to the lipid phosphatidylethanolamine (PE) upon interaction with autophagic membranes (Kouno *et al.* 2005). Atg8/LC3 remains bound to autophagic membranes until degradation in lysosomes, thus serving as a useful marker of autophagy (Ohsumi 2001). In yeast and flies, Atg1 is required for autophagosome biogenesis and is found on preautophagic and autophagic double-membrane structures together with Atg18 (Reggiori *et al.* 2004; Scott *et al.* 2004). Mutations in both Drosophila *atg1* and *atg18* have been shown to block starvation-induced autophagy in larval fat body tissue (Scott *et al.* 2004). For our assay, enhancement of the dominant eye phenotype likely indicates that a decreased level of key autophagy components in conjunction with excess Bchs exacerbates the GOF eye defects. At this time the cellular mechanism of this enhancement is unclear but may involve defects with autophagic vesicle formation or global perturbation of microtubule-mediated transport of membrane vesicles.

Modifying mutations in AP-3 complex and late endosomal genes: Although endogenous Bchs is not expressed in pigment cells and functional loss of Bchs does not alter pigment granule formation (data not shown), mutations that affect eye and body pigmentation were examined because pigment vesicles or granules originate as part of the lysosomal biogenesis pathway. Several genes involved with lysosomal and pigment granule biogenesis acted as strong Bchs-GOF modifiers. They include the four subunits of the Drosophila AP-3 adaptor complex, which mediate trafficking between the *trans*-Golgi network and lysosomes (Boehm and Bonifacino 2002). Mutations in *orange* (ξ-subunit, Figure 4g) and *ruby* (β-subunit, Figure 4h) are strong enhancers while alterations to *garnet* (δ-subunit, Figure 4i) and *carmine* (μ-subunit, Figure 4j) behave as complex modifiers by enhancing pigmentation defects and suppressing the eye size reduction (Lloyd *et al.* 1998). A decrease in pigmentation suggests that expression of Bchs in pigment cells (where it is normally not expressed) has a deleterious effect on pigment granule formation.

Spinster mutations also behave as enhancers of the Bchs-GOF eye phenotype (Figure 4k). Encoding an integral membrane protein, hypomorphic *spinster* alleles were first identified having adult behavior and neural development defects (Nakano *et al.* 2001). More recently, *spinster* (*benchwarmer*) mutants demonstrated neural degeneration accompanied by the formation of late endosomal inclusions (Dermaut *et al.* 2005). Localized to lysosomes and late endosomes the vertebrate spinster protein promotes the autophagic cell death pathway in cultured cells (Yanagisawa *et al.* 2003). Mutations in other genes classified with late endosomal/lysosomal functions also act as Bchs-GOF enhancers. They include *deep orange* (*dor*, Vps18p, E3-ligase, Figure 4l) and *carnation* (Vps33, sec1 protein, Figure 4m) (Sevrioukov *et al.* 1999). These proteins are members of the *ho*meotypic vacuole fusion and *p*rotein *s*orting (HOPS) trafficking complex and in Drosophila are known to promote late endosomal/lysosomal fusion events (Sriram *et al.* 2003). Recently we demonstrated that, like its yeast homolog Vps18p, Drosophila *dor* is required for autophagosome-to-lysosome fusion during programmed autophagy in the larval fat body (Lindmo *et al.* 2006). Mutant alleles of a second Sec1 protein, *ras opposite* (*rop*, munc-18/n-Sec1) enhance the Bchs-GOF phenotype (Figure 4n) as do mutant alleles of *syntaxin1A*, *syntaxin13*, and the coiled-coil protein *hook* (Figure 4, o and p) (FlyBase 2007). Drosophila *hook* is known to genetically interact with *dor* during endocytosis by regulating multivesicular endosome (MVE) trafficking (Figure 4q) (Narayanan *et al.* 2000). Both hook and dor proteins are found in larval neuromuscular synapses and mutations in both alter synaptic size and number (increased in *hook* and decreased in *dor*) (Narayanan *et al.* 2000). Ras opposite, syntaxin1A, and syntaxin 13 are SNARE proteins that are involved in neurotransmitter release (Ciufo *et al.* 2005).

Another important class of proteins involved in regulating vesicle trafficking and fusion is Rab GTPases. Several independent mutations in *Rab11* (Figure 4r) act as very strong enhancers of the Bchs-GOF phenotype. Rab11 is known to associate with multiple vesicle subtypes ranging from recycling endosomes to *trans*-Golgi vesicles and has important roles in endocytosis (recycling and lysosomal targeting) and membrane targeting during cytokinesis and cellularization (Pelissier *et al.* 2003). The potential genetic interaction between *Rab11* and *Bchs* was recently confirmed in a similar study that examined their combinatorial effect on synaptic development and morphogenesis (Khodosh *et al.* 2006). In the Drosophila eye, Rab11 also mediates rhodopsin exocytosis and prevents photoreceptor degeneration (Satoh *et al.* 2005). Additional genes involved with the biogenesis of lysosomes and related organelles were also identified as having potential interactions with Bchs. They include a second *rab* gene, *lightoid* (Figure 4s) and *claret*, a GTPases guanine nucleotide exchange factor (Figure 4t) (Ma *et al.* 2004). These two proteins are known to interact and promote the formation of pigment granules during eye development (Ma *et al.* 2004).

Cytoskeletal/motor proteins and ubiquitin/SUMO pathway member modifiers: Recent studies examining the removal of aggregate-prone proteins revealed that microtubules and motor proteins are required for appropriate formation and trafficking of autophagosomes (Kamal and Goldstein 2000; Ravikumar *et al.* 2005) and point mutations in human dynein result in an ALS-like form of neuronal degeneration. Since Bchs contains potential motifs implicated in interactions with motor and cytoskeleton proteins we therefore assayed mutations in this class of genes. The Bchs-GOF phenotype

was significantly enhanced by mutations in the *dynein light chain* (*DLC*, Figure 4u) and α-*tubulin* (Figure 4w) genes and to a lesser extent with the *dynein heavy chain* gene (*DHC*, Figure 4v) (FlyBase 2007). β-*tubulin* mutations did not show a significant change in the overall Bchs-GOF phenotype (Figure 4x) as do other functionally related genes (*i.e.*, actin). Since *bchs* mutant flies demonstrate age-related changes to CNS ubiquitinated protein profiles, genes in the ubiquitin and SUMO signaling pathways were also assayed (Finley *et al.* 2003). While its unknown if Bchs interacts directly with ubiquitin or SUMO, ubiquitin/SUMO signaling has profound effects on vesicle specification and trafficking to lysosomes and both can be major constituents of cellular inclusions (Steffan *et al.* 2004; Ciechanover 2005). Mutant alleles of the Drosophila *SUMO* gene (smt3, Figure 4y) enhance the Bchs-GOF phenotype as do mutations in the SUMO-conjugating enzyme *lesswright* (*lwr*, Figure 4z) (FlyBase 2007). Mutations in fly *Uba* (ubiquitin-activating enzyme 1, Figure 4aa), a C-terminal ubiquitin hydrolase (CG1490, Figure 4bb) and *effete* (UbcD1, ubiquitin-conjugating enzyme 1, Figure 4cc) also are Bchs-GOF enhancers (Ohlmeyer and Schupbach 2003).

Adult life span profiles of Bchs modifiers: A key phenotype associated with functional loss of *bchs* in adult Drosophila is a significant reduction in longevity. We therefore asked if genes with potential genetic interactions with *bchs* demonstrate a similar LOF phenotype. To test this hypothesis, we examined the life span of mutations that were identified by the Bchs modifier screen. Fortunately, several mutant alleles exist that produce homozygous viable adults with normal appearance and activity levels. To control for genetic background effects related to life span, mutant lines were first outcrossed for several generations to wild-type stocks (Canton-S or w^{1118}) and independent lines were reestablished for these studies. The $hook^{1}$ and $hook^{11}$ lines were assayed independently from each other and in heterozygous combination ($hook^{1}/hook^{11}$). Newly emerged adults were collected and aged to determine the life span profiles for *deep orange*, *light*, *carnation*, *hook*, *ruby*, *garnet*, *carmine*, and *atg8a* mutants at both 25° and 29° (Figure 5, a and b). The results are summarized in Table 2 (Finley *et al.* 2003). Canton-S and w^{1118} and $rosy^{26}$ strains were used as normal and eye pigment mutant controls (FlyBase 2007).

The mutants that demonstrated the shortest average life span were weak alleles of *deep orange* (Figure 5a) (FlyBase 2007). Both male and female dor^{1} flies and dor^{4} males showed similar aging profiles, with nearly all dead within 16 days (Table 2). $Carnation^{1}$ and $hook^{1}$ mutants also have a significant life span reduction when compared to controls. Previous work has found that $hook^{1}$ mutants develop retinal degeneration (Kramer and Phistry 1996) and this study shows that $hook^{1}$ and $hook^{1}/hook^{11}$ *trans*-heterozygous flies have decreased longevity

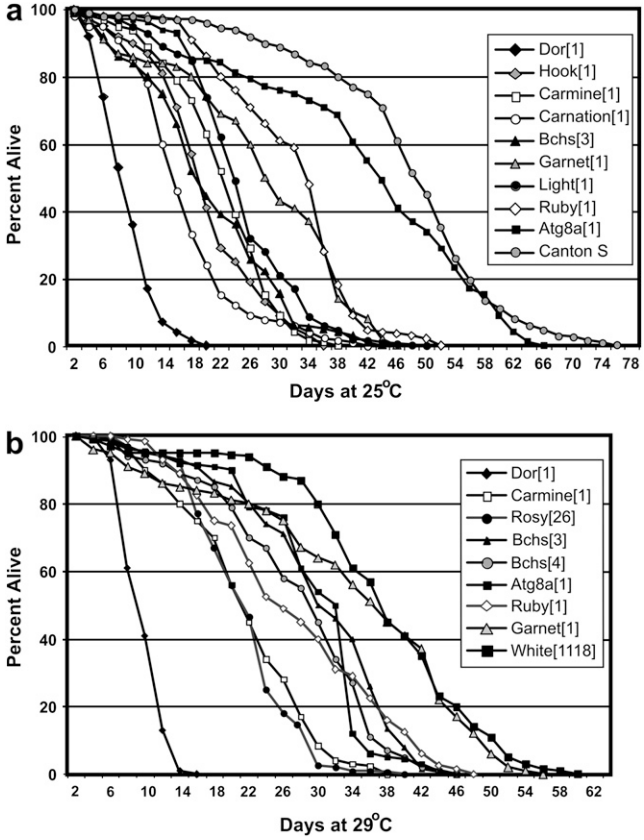

Figure 5.—Life span profiles of Bchs modifiers. Newly eclosed males from different genotypes were collected and aged at (a) 25° and (b) 29° for the duration of the experiment. The percentage of individuals for a given genotype that had survived for a given day is calculated from the total number of flies. For each genotype the total number of flies (*n*) used in the experiment, their mean life spans, standard deviations, and *P*-values are summarized in Table 2A and 2B.

profiles similar to *bchs* adults (Table 2). Several mutant lines have average life spans greater than *bchs* mutants, but still significantly less than control lines. At 25° they include *light*, *carmine*, *ruby*, and *garnet* mutations, as well as a *P*-element insertion into the *atg8a* gene (Figure 5a). Most mutants have similar profiles when compared at 25° and 29°. The exceptions are $rosy^{26}$, which has a significant decrease in longevity at 29°, and $garnet^{1}$ mutants that have a nearly normal life span (Figure 5b). While these lysosomal trafficking mutants have been studied extensively in terms of synaptic vesicle function and pigment granule development, to our knowledge this is the first detailed examination of their life span profiles. Our results clearly show that mutations in lysosomal trafficking proteins can reduce adult longevity.

To determine if mutations in *bchs* and other lysosomal trafficking genes have an additive effect on adult phenotypes we established crosses between different allelic combination of *bchs* and other lysosomal trafficking mutants. Unfortunately, the combination of strong deletion alleles of *bchs* [*Df(2L)dsf3/Df(2L)clot7* or *Df(2L)dsf3/Df(2)w3*] with several lysosomal genes produced very

TABLE 2

Adult life span profiles

Genotype	Gender	Total (*n*)	Mean age (days)	SD[a]	Maximum age (days)	*P*-value
			A. At 25°			
dor^{1}	Male	295	8.96	3.73	20	<0.0001[b]
dor^{1}	Female	98	10.07	3.62	15	<0.0001[b]
dor^{4}	Male	106	13.94	2.95	19	<0.0001[b]
hook^{1}/*hook*^{11}	Male	110	18.76	8.27	58	<0.0001[b]
hook^{1}	Male	338	19.861	7.26	36	<0.0001[b]
carnation^{1}	Male	242	17.42	8.69	48	<0.0001[b]
bchs^{3}/*df clot7*	Male	330	21.69	10.54	46	<0.0001[b]
bchs^{3}/*bchs*^{5}	Male	274	23.7	6.9	37	<0.0001[b]
carmine^{1}	Male	351	21.97	6.96	38	<0.0001[b]
light^{1}	Male	247	24.92	8.8	61	<0.0001[b]
garnet^{1}	Male	111	27.41	11.75	45	<0.0001[b]
ruby^{1}	Male	183	31.57	8.842	53	0.0001[b]
atg8a^{ep362}	Male	150	41.9	15.4	66	0.0040[b]
Canton-S	Male	264	46.85	12.33	68	
			B. At 29°			
deep orange^{1}	Male	136	8.19	2.4	14	<0.0001[c]
rosy^{26}	Male	128	19.8	5.98	38	<0.0001[c]
carmine^{1}	Male	122	20.69	7.73	36	<0.0001[c]
carnation^{1}	Male	121	23.868	8.78	42	<0.0001[c]
bchs^{3}/*bchs*^{6}	Male	156	20.08	6.74	36	<0.0001[c]
bchs^{3}/*Df(2L)clot7*	Male	80	22.23	6.3	32	<0.0001[c]
bchs^{4} *(EP2299)*	Male	196	25.87	9.09	44	<0.0001[c]
agt8a^{1}	Male	153	27.16	7.732	45	<0.0001[c]
garnet^{1}	Male	98	32.08	13.84	54	0.0194[c]
white^{1118}	Male	124	36.02	10.97	58	

[a] Standard deviation from the mean.
[b] *P*-values were calculated using Canton-S as a control.
[c] *P*-values were calculated using *white* ^{1118} as a control.

few double-mutant adults (Finley *et al.* 1998, 2003). Using other *bchs* mutant alleles we were able to generate an occasional double-mutant male fly by combining the *bchs*^{5}/*Df(2L)dsf3* genotype individually with the *dor*^{1}, *ruby*^{1}, *carnation*^{1}, *atg8a*^{2}, *garnet*^{1}, and *carmine*^{1} mutations (scored for eye color). Again, eclosion rates for the different *bchs*^{5}/*Df(2L)dsf3* genetic combinations were substantially reduced but a few viable flies were produced. Heads were harvested from 1- to 2-day-old animals and protein extracts were examined by Western blot analysis. Since *bchs* LOF mutations do not produce an easy-to-score phenotype we confirmed functional loss of *bchs* by Western analysis (anti-Bchs) in conjunction with total UB-protein profiles (Figure 3b). As seen previously, *bchs* mutants [*bchs*^{5}/*Df(2L)dsf3*] have an elevated UB-protein level when compared to age-matched controls (Canton-S). A similar elevation in large UB proteins was also detected for *ruby*^{1}, *carnation*^{1}, and *atg8a*^{2} single mutants. This phenotype was further exacerbated in double mutants with the *bchs*^{5}/*Df(2L)dsf3* genotype. An increase in UB-protein levels was detected for *garnet*^{1} and *carmine*^{1} mutant males but was not detected in *garnet*^{1};*bchs*^{5}/*Df(2L)dsf3* and *carmine*^{1};*bchs*^{5}/*Df(2L)dsf3* double mutants (data not shown). These data indicate that individual mutations in *bchs* or other genes involved with lysosomal transport/trafficking can alter UB-protein profiles in young adult neural tissues and in several examples double-mutant combinations produce an additive or synergistic phenotype.

DISCUSSION

Lysosomal-autophagic trafficking defects: There is growing evidence that defects in lysosomal transport or clearance of age-related or disease-associated proteins can play a central role in the etiology of many neural degenerative disorders (Cataldo *et al.* 1996; Garcia-Mata *et al.* 2002; Ravikumar *et al.* 2005; Yu *et al.* 2005). Previous work on Bchs and Alfy indicated that these proteins are involved with the autophagic clearance of ubiquitinated substrates. Human Alfy colocalizes with cytoplasmic ubiquitin structures and autophagic membranes and older *bchs* mutant flies accumulate ubiquitinated CNS aggregates (Finley *et al.* 2003; Simonsen *et al.* 2004). In this study we show that high levels of Bchs in the Drosophila eye cause a dominant eye phenotype in which external eye structures and neural development are perturbed (Figure 2). Neural defects include

alterations to the formation of terminal synapses and axonal varicosities containing ubiquitin. Biochemical analysis reveals that both *bchs* mutant and overexpressing flies show similar changes in UB-protein profiles (Figure 3). These phenotypes suggest that lysosomal transport defects alter the turnover of UB proteins (Gunawardena and Goldstein 2001; Nixon *et al.* 2005). A Bchs-GOF screen was designed around this overexpression eye phenotype and used to identify several candidate proteins (modifiers) that potentially have genetic interactions with Bchs.

The role of lysosomal mutations in adult viability: Several loss-of-function mutations within the autophagic pathway were found to behave as Bchs-GOF enhancers (*Atg1* and *Atg6*), while two transgenic lines that allow *GMR-Gal4*-driven coexpression with *EP(2L)2299* (*UAS-atg2* and *UAS-atg8a*) mildly suppress a dominant eye phenotype. This is similar to previous findings with *GMR-Gal4* expression of *UAS-SNAP* in which the genetic background of known interacting factors enhanced or suppressed the dominant eye phenotype (Babcock *et al.* 2004). Other classes of proteins that are involved with different aspects of lysosomal transport also act as Bchs-GOF modifiers, including the four subunits of the AP-3 protein complex (*orange*, *ruby*, *garnet*, and *carmine*). These four protein subunits have primarily been characterized in terms of pigment granule biosynthesis but clearly they have additional cellular functions since all are located within Drosophila nerve terminals and have a subtle role in adult behaviors (Dell'Angelica *et al.* 2000; Boehm and Bonifacino 2002). Lysosomal trafficking and pigmentation defects are also observed with mutant mammalian AP-3 homologs. Mutant mocha (δ-subunit) and pearl (β3A-subunit) mice have pigmentation defects and lysosomal abnormalities as do humans suffering from Hermansky–Pudlak syndrome (β3A-subunit) (Dell'Angelica *et al.* 2000; Boehm and Bonifacino 2002). In addition, mocha mice demonstrate progressive inner ear and neurological degeneration.

Several proteins characterized as having roles in the late endosomal pathway were scored as positive Bchs-GOF eye modifiers including mutations in the *spinster*, *hook*, *deep orange*, and *carnation* genes. Drosophila mutations in these genes have been shown to affect neuronal maintenance and degeneration. Defects in the mouse and human homologs of *carnation* (Vps33) generate *buff* mutant mice and the ARC syndrome in humans (Vps33B, lethal multisystem disorder), respectively (Gissen *et al.* 2004). Previously we have shown that, in addition to the late endosomal–lysosomal fusion events, the Deep orange protein also facilitates the formation of autolysosmes (autophagosome–lysosome vesicles) or amphisomes (autophagosome–late endosome vesicles) (Rieder and Emr 1997; Lindmo *et al.* 2006). Other known "lysosomal" proteins that mediate a host of trafficking/fusion events in several vesicle subtypes were also scored as Bchs-GOF modifiers. These include *ras opposite*, *syntaxin1A*, *syntaxin13*, *Rab11*, *lightoid*, *claret*, α-*tubulin*, and the *dynein light chain* mutations. Defects in dynein-mediated transport are linked with neurodegenerative disorders and recently were shown to impair autophagy-mediated clearance of neuronal protein aggregates (Ravikumar *et al.* 2005).

The addition of ubiquitin to protein substrates is used by the cell as a signal for proteasome degradation or as a sorting signal for endocytotic trafficking to the lysosome. The accumulation of ubiquitinated-protein aggregates or inclusions is a key feature of many neural degenerative disorders and is a primary phenotype associated with *bchs* loss-of-function mutations. More recently SUMOylated proteins have also been found in neural inclusions, indicating that multiple changes in protein modification, trafficking, and/or proteolytic turnover pathways can be a central feature of neural degeneration and reduced viability (Steffan *et al.* 2004). In our study mutations in both the SUMO (*SUMO* and *lesswright*) and ubiquitin (*uba*, *CG1490*, and *effete*) pathways behaved as enhancers of the Bchs-GOF phenotype. At this time it remains unclear if this is due to direct interactions between the Bchs protein and ubiqutinated or SUMOylated substrates or to a general blockage in vesicle sorting and transport.

Deletion lines and negative modifiers indicate screen selectivity: In this study we identified eight regional deletions that behave as Bchs modifiers, which removed individual genes that were also scored as modifiers (Table 1, underlined). The remaining 11 Bchs-modifier genes located on the second and the third chromosome were eliminated by a deletion interval that did not generate a phenotype meeting the criteria set as being sufficiently significant. This discrepancy may be related to the level of modification produced by an individual mutation. In our screen and in a separate study (Khodosh *et al.* 2006) *Rab11* mutations show a pronounced unambiguous eye phenotype that corresponds well with regional deletions. A similar strong phenotype was also seen with the *lightoid* mutations (Figure 4s) where either a single mutation or elimination of its genomic region resulted in obvious modification of the eye. This implies that an intermediate phenotype may be masked by the removal of other genes in the region that act as even moderate suppressors. A moderate suppression could involve the loss of a direct interaction between a trafficking protein and Bchs or the removal of transcription factors that normally enhance the endogenous *bchs* gene expression or have an upstream effect on the Gal4/UAS-driven expression. Although the deletion screen was informative the direct testing of individual genes helped to more quickly narrow the focus of this study.

Information regarding Bchs's functional pathway was also obtained from mutations that had little or no effect on the dominant Bchs-GOF eye phenotype. For a complete list of mutations that were tested and determined not to modify the Bchs eye phenotype see supplemental

Table 3 at http://www.genetics.org/supplemental/. Eye-pigment mutants that are members of the ABC transporter class of lysosomal proteins (*white*, *brown*, and *scarlet*) did not modify the Bchs-GOF phenotype nor did genes that have early endosomal functions like *hrs*, *clatherin-HC*, or *lap* (AP180-like protein) (FlyBase 2007). Additional genes in vesicle trafficking pathways were also tested and mutations in *sec61α*, *synaptotagmin*, *doa*, *rph*, *rab5*, and *rab14* genes did not produce significant modification of the Bchs eye phenotype (data not shown) (FlyBase 2007). Since insulin/TOR signaling is known to regulate autophagy, members of this pathway were examined for Bchs interactions (Kapahi *et al.* 2004; Ravikumar *et al.* 2004). Mutations in *chico* (insulin-like receptor), *InR*, and *Tor* genes did not have a significant effect on the Bchs-GOF phenotype (Kapahi *et al.* 2004). This may indicate a lack of direct protein interactions with Bchs or that a second signaling pathway regulates different features of autophagy regarding aggregate clearance in neurons. Kinesin motor proteins play a major role in vesicle trafficking and several mutations in kinesin and kinesin-like genes were examined and none produced a significant change in the Bchs-GOF phenotype. Finally, not all members of the ubiquitin-signaling pathway acted as Bchs modifiers, including mutations in *Ubp64E*, *Uch-L3*, *fat facets*, *UbcD 10*, and *UbcD4*. The fact that only certain genes in lysosomal trafficking pathways acted as Bchs-GOF modifiers highlights the interaction specificity of the screen's design. It also indicates that Bchs may preferentially interact with proteins involved in late transport events to the lysosome or the autophagic-to-lysosomal or *trans*-Golgi/late endosomal-to-lysosomal transport processes.

Decreased longevity and UB-protein accumulation in lysosomal trafficking mutants: Lysosomal trafficking defects are often associated with progressive disorders and reduced viability (Cataldo *et al.* 1996; Dell'Angelica *et al.* 2000; Brunk and Terman 2002; Cuervo 2004). To further clarify the role that lysosomal transport has on the adult Drosophila life span, mutant lines identified from the modifier screen were examined for changes in adult longevity. We found that mutations in several AP-3 genes (*ruby*, *garnet*, and *carmine*), late endosomal pathway genes (*i.e.*, *deep orange*, *carnation*, and *hook*), and the autophagy gene *atg8a* resulted in reduced average adult life spans. While the decrease in longevity associated with *bchs* mutations can be attributed to progressive neural defects this may not be the case for mutations in other lysosomal import genes. Bchs is primarily expressed in neurons while the other genes have a broader expression pattern (Finley *et al.* 2003). For example we have shown that *dor* (described as an endosomal gene) is required for programmed autophagy in larval fat body cells (Lindmo *et al.* 2006). This suggests that lysosomal defects in nonneuronal tissues may also contribute to premature adult death associated with these mutants (Lindmo *et al.* 2006). However, a preliminary examination of UB proteins from mutant flies shows that most genotypes demonstrate a pronounced accumulation of proteins. In addition, several double-mutant combinations with *bchs* show an additive effect on UB-protein levels, with the most striking effect occurring with dor^1 and $carnation^1$ mutations. While both proteins are known to genetically interact and closely associate during late endosomal trafficking we have recently shown that the Dor protein functions during the activation of the programmed autophagic pathway in the larval fat body. The implications are that individual proteins may have dual functions, which reflect tissue-specific or age-dependent requirements coming from different lysosomal trafficking pathways.

Conclusion: The genetic analysis of *bchs* interactions further supports the hypothesis that Bchs serves as a large scaffolding protein with multiple interacting partners. These genetic interactions primarily involve genes known to promote the transport, targeting, or fusion of different vesicle subpopulations with the lysosome. Viable loss-of-function mutations in autophagic, *trans*-Golgi, and late endosomal pathway members produce subtle but progressive defects that decrease adult longevity by altering the transport of substrates to the lysosome. Furthermore, our Drosophila genetic findings have implications for human disease since each gene characterized in this study has a direct human homolog and several are associated with diseases characterized by defects in lysosomal trafficking or function (FlyBase 2007). Many others have not been directly linked to a human disease but several map to loci associated with progressive disorders. Using Drosophila as an efficient model system, these genes and phenotypic defects can become a focus for future studies related to human disorders.

We thank Kia Zinn for providing the Bchs antibody, Helmut Kramer for the $hook^{11}$ allele, and the Bloomington Stock Center for the remainder of the mutant lines examined in this study. This work was supported by grants from the National Institutes of Health, the National Institute on Aging, the National Institute on Neurological Disorders and Stroke (K.F. and R.C.), and the Norwegian Cancer Society (A.S. and K.L.) and by the Research Council of Norway (T.R.).

LITERATURE CITED

Babcock, M., G. T. Macleod, J. Leither and L. Pallanck, 2004 Genetic analysis of soluble N-ethylmaleimide-sensitive factor attachment protein function in Drosophila reveals positive and negative secretory roles. J. Neurosci. **24:** 3964–3973.

Bjorkoy, G., T. Lamark, A. Brech, H. Outzen, M. Perander *et al.*, 2005 p62/SQSTM1 forms protein aggregates degraded by autophagy and has a protective effect on huntingtin-induced cell death. J. Cell Biol. **171:** 603–614.

Boehm, M., and J. S. Bonifacino, 2002 Genetic analyses of adaptin function from yeast to mammals. Gene **286:** 175–186.

Brunk, U. T., and A. Terman, 2002 The mitochondrial-lysosomal axis theory of aging: accumulation of damaged mitochondria as a result of imperfect autophagocytosis. Eur. J. Biochem. **269:** 1996–2002.

Cataldo, A. M., D. J. Hamilton, J. L. Barnett, P. A. Paskevich and R. A. Nixon, 1996 Properties of the endosomal-lysosomal system in the human central nervous system: disturbances mark most neurons in populations at risk to degenerate in Alzheimer's disease. J. Neurosci. **16:** 186–199.

Ciechanover, A., 2005 Proteolysis: from the lysosome to ubiquitin and the proteasome. Nat. Rev. Mol. Cell. Biol. **6:** 79–87.

Ciufo, L. F., J. W. Barclay, R. D. Burgoyne and A. Morgan, 2005 Munc18–1 regulates early and late stages of exocytosis via syntaxin-independent protein interactions. Mol. Biol. Cell **16:** 470–482.

Cuervo, A. M., 2004 Autophagy: in sickness and in health. Trends Cell Biol. **14:** 70–77.

Dell'Angelica, E. C., C. Mullins, S. Caplan and J. S. Bonifacino, 2000 Lysosome-related organelles. FASEB J. **14:** 1265–1278.

Dermaut, B., K. K. Norga, A. Kania, P. Verstreken, H. Pan *et al.*, 2005 Aberrant lysosomal carbohydrate storage accompanies endocytic defects and neurodegeneration in Drosophila benchwarmer. J. Cell Biol. **170:** 127–139.

Ditch, L. M., T. Shirangi, J. L. Pitman, K. L. Latham, K. D. Finley *et al.*, 2005 Drosophila retained/dead ringer is necessary for neuronal pathfinding, female receptivity and repression of fruitless independent male courtship behaviors. Development **132:** 155–164.

Fernandez-Funez, P., M. L. Nino-Rosales, B. de Gouyon, W. C. She, J. M. Luchak *et al.*, 2000 Identification of genes that modify ataxin-1-induced neurodegeneration. Nature **408:** 101–106.

Finley, K. D., P. T. Edeen, M. Foss, E. Gross, N. Ghbeish *et al.*, 1998 Dissatisfaction encodes a tailless-like nuclear receptor expressed in a subset of CNS neurons controlling Drosophila sexual behavior. Neuron **21:** 1363–1374.

Finley, K. D., P. T. Edeen, R. C. Cumming, M. D. Mardahl-Dumesnil, B. J. Taylor *et al.*, 2003 blue cheese mutations define a novel, conserved gene involved in progressive neural degeneration. J. Neurosci. **23:** 1254–1264.

FlyBase, 2007 http://flybase.bio.indiana.edu.

Garcia-Mata, R., Y. S. Gao and E. Sztul, 2002 Hassles with taking out the garbage: aggravating aggresomes. Traffic **3:** 388–396.

Gissen, P., C. A. Johnson, N. V. Morgan, J. M. Stapelbroek, T. Forshew *et al.*, 2004 Mutations in VPS33B, encoding a regulator of SNARE-dependent membrane fusion, cause arthrogryposis-renal dysfunction-cholestasis (ARC) syndrome. Nat. Genet. **36:** 400–404.

Greaves, S., B. Sanson, P. White and J. P. Vincent, 1999 A screen for identifying genes interacting with armadillo, the Drosophila homolog of β-catenin. Genetics **153:** 1753–1766.

Gunawardena, S., and L. S. Goldstein, 2001 Disruption of axonal transport and neuronal viability by amyloid precursor protein mutations in Drosophila. Neuron **32:** 389–401.

Hara, T., K. Nakamura, M. Matsui, A. Yamamoto, Y. Nakahara *et al.*, 2006 Suppression of basal autophagy in neural cells causes neurodegenerative disease in mice. Nature **441:** 885–890.

Kamal, A., and L. S. Goldstein, 2000 Connecting vesicle transport to the cytoskeleton. Curr. Opin. Cell Biol. **12:** 503–508.

Kapahi, P., B. M. Zid, T. Harper, D. Koslover, V. Sapin *et al.*, 2004 Regulation of lifespan in Drosophila by modulation of genes in the TOR signaling pathway. Curr. Biol. **14:** 885–890.

Kazemi-Esfarjani, P., and S. Benzer, 2000 Genetic suppression of polyglutamine toxicity in Drosophila. Science **287:** 1837–1840.

Khodosh, R., A. Augsburger, T. L. Schwarz and P. A. Garrity, 2006 Bchs, a BEACH domain protein, antagonizes Rab11 in synapse morphogenesis and other developmental events. Development **133:** 4655–4665.

Klionsky, D. J., and S. D. Emr, 2000 Autophagy as a regulated pathway of cellular degradation. Science **290:** 1717–1721.

Klionsky, D. J., J. M. Cregg, W. A. Dunn, Jr., S. D. Emr, Y. Sakai *et al.*, 2003 A unified nomenclature for yeast autophagy-related genes. Dev. Cell **5:** 539–545.

Komatsu, M., S. Waguri, T. Ueno, J. Iwata, S. Murata *et al.*, 2005 Impairment of starvation-induced and constitutive autophagy in Atg7-deficient mice. J. Cell Biol. **169:** 425–434.

Komatsu, M., S. Waguri, T. Chiba, S. Murata, J. I. Iwata *et al.*, 2006 Loss of autophagy in the central nervous system causes neurodegeneration in mice. Nature **441:** 880–884.

Kouno, T., M. Mizuguchi, I. Tanida, T. Ueno, T. Kanematsu *et al.*, 2005 Solution structure of microtubule-associated protein light chain 3 and identification of its functional subdomains. J. Biol. Chem. **280:** 24610–24617.

Kramer, H., and M. Phistry, 1996 Mutations in the Drosophila hook gene inhibit endocytosis of the boss transmembrane ligand into multivesicular bodies. J. Cell Biol. **133:** 1205–1215.

Kramer, H., and M. Phistry, 1999 Genetic analysis of hook, a gene required for endocytic trafficking in Drosophila. Genetics **151:** 675–684.

Kraut, R., K. Menon and K. Zinn, 2001 A gain-of-function screen for genes controlling motor axon guidance and synaptogenesis in Drosophila. Curr. Biol. **11:** 417–430.

Lindmo, K., A. Simonsen, A. Brech, K. Finley, T. E. Rusten *et al.*, 2006 A dual function for Deep orange in programmed autophagy in the Drosophila melanogaster fat body. Exp. Cell Res. **312:** 2018–2027.

Lloyd, V., M. Ramaswami and H. Kramer, 1998 Not just pretty eyes: Drosophila eye-colour mutations and lysosomal delivery. Trends Cell Biol. **8:** 257–259.

Luzio, J. P., P. R. Pryor, S. R. Gray, M. J. Gratian, R. C. Piper *et al.*, 2005 Membrane traffic to and from lysosomes. Biochem. Soc. Symp. No. 72, 77–86.

Ma, J., H. Plesken, J. E. Treisman, I. Edelman-Novemsky and M. Ren, 2004 Lightoid and Claret: a rab GTPase and its putative guanine nucleotide exchange factor in biogenesis of Drosophila eye pigment granules. Proc. Natl. Acad. Sci. USA **101:** 11652–11657.

Nakano, Y., K. Fujitani, J. Kurihara, J. Ragan, K. Usui-Aoki *et al.*, 2001 Mutations in the novel membrane protein spinster interfere with programmed cell death and cause neural degenerationin Drosophila melanogaster. Mol. Cell. Biol. **21:** 3775–3788.

Narayanan, R., H. Kramer and M. Ramaswami, 2000 Drosophila endosomal proteins hook and deep orange regulate synapse size but not synaptic vesicle recycling. J. Neurobiol. **45:** 105–119.

Nixon, R. A., J. Wegiel, A. Kumar, W. H. Yu, C. Peterhoff *et al.*, 2005 Extensive involvement of autophagy in Alzheimer disease: an immuno-electron microscopy study. J. Neuropathol. Exp. Neurol. **64:** 113–122.

Ohlmeyer, J. T., and T. Schupbach, 2003 Encore facilitates SCF-Ubiquitin-proteasome-dependent proteolysis during Drosophila oogenesis. Development **130:** 6339–6349.

Ohsumi, Y., 2001 Molecular dissection of autophagy: two ubiquitin-like systems. Nat. Rev. Mol. Cell. Biol. **2:** 211–216.

Pelissier, A., J. P. Chauvin and T. Lecuit, 2003 Trafficking through Rab11 endosomes is required for cellularization during Drosophila embryogenesis. Curr. Biol. **13:** 1848–1857.

Pitman, J. L., C. C. Tsai, P. T. Edeen, K. D. Finley, R. M. Evans *et al.*, 2002 DSF nuclear receptor acts as a repressor in culture and in vivo. Dev. Biol. **245:** 315–328.

Raiborg, C., T. E. Rusten and H. Stenmark, 2003 Protein sorting into multivesicular endosomes. Curr. Opin. Cell Biol. **15:** 446–455.

Ravikumar, B., C. Vacher, Z. Berger, J. E. Davies, S. Luo *et al.*, 2004 Inhibition of mTOR induces autophagy and reduces toxicity of polyglutamine expansions in fly and mouse models of Huntington disease. Nat. Genet. **36:** 585–595.

Ravikumar, B., A. Acevedo-Arozena, S. Imarisio, Z. Berger, C. Vacher *et al.*, 2005 Dynein mutations impair autophagic clearance of aggregate-prone proteins. Nat. Genet. **37:** 771–776.

Rebay, I., F. Chen, F. Hsiao, P. A. Kolodziej, B. H. Kuang *et al.*, 2000 A genetic screen for novel components of the Ras/Mitogen-activated protein kinase signaling pathway that interact with the yan gene of Drosophila identifies split ends, a new RNA recognition motif-containing protein. Genetics **154:** 695–712.

Reggiori, F., K. A. Tucker, P. E. Stromhaug and D. J. Klionsky, 2004 The Atg1-Atg13 complex regulates Atg9 and Atg23 retrieval transport from the pre-autophagosomal structure. Dev. Cell **6:** 79–90.

Rieder, S. E., and S. D. Emr, 1997 A novel RING finger protein complex essential for a late step in protein transport to the yeast vacuole. Mol. Biol. Cell **8:** 2307–2327.

Rorth, P., 1996 A modular misexpression screen in Drosophila detecting tissue-specific phenotypes. Proc. Natl. Acad. Sci. USA **93:** 12418–12422.

Satoh, A. K., J. E. O'Tousa, K. Ozaki and D. F. Ready, 2005 Rab11 mediates post-Golgi trafficking of rhodopsin to the photosensitive apical membrane of Drosophila photoreceptors. Development **132:** 1487–1497.

Scott, R. C., O. Schuldiner and T. P. Neufeld, 2004 Role and regulation of starvation-induced autophagy in the Drosophila fat body. Dev. Cell **7:** 167–178.

Sevrioukov, E. A., J. P. He, N. Moghrabi, A. Sunio and H. Kramer, 1999 A role for the deep orange and carnation eye color genes in lysosomal delivery in Drosophila. Mol. Cell **4:** 479–486.

Shih, S. C., D. J. Katzmann, J. D. Schnell, M. Sutanto, S. D. Emr *et al.*, 2002 Epsins and Vps27p/Hrs contain ubiquitin-binding domains that function in receptor endocytosis. Nat. Cell. Biol. **4:** 389–393.

Shulman, J. M., and M. B. Feany, 2003 Genetic modifiers of tauopathy in Drosophila. Genetics **165:** 1233–1242.

Simonsen, A., H. C. Birkeland, D. J. Gillooly, N. Mizushima, A. Kuma *et al.*, 2004 Alfy, a novel FYVE-domain-containing protein associated with protein granules and autophagic membranes. J. Cell Sci. **117:** 4239–4251.

Sriram, V., K. S. Krishnan and S. Mayor, 2003 deep-orange and carnation define distinct stages in late endosomal biogenesis in Drosophila melanogaster. J. Cell Biol. **161:** 593–607.

Steffan, J. S., N. Agrawal, J. Pallos, E. Rockabrand, L. C. Trotman *et al.*, 2004 SUMO modification of Huntingtin and Huntington's disease pathology. Science **304:** 100–104.

Torroja, L., H. Chu, I. Kotovsky and K. White, 1999 Neuronal overexpression of APPL, the Drosophila homologue of the amyloid precursor protein (APP), disrupts axonal transport. Curr. Biol. **9:** 489–492.

Verheyen, E. M., K. J. Purcell, M. E. Fortini and S. Artavanis-Tsakonas, 1996 Analysis of dominant enhancers and suppressors of activated Notch in Drosophila. Genetics **144:** 1127–1141.

Yanagisawa, H., T. Miyashita, Y. Nakano and D. Yamamoto, 2003 HSpin1, a transmembrane protein interacting with Bcl-2/Bcl-xL, induces a caspase-independent autophagic cell death. Cell Death Differ. **10:** 798–807.

Yu, W. H., A. M. Cuervo, A. Kumar, C. M. Peterhoff, S. D. Schmidt *et al.*, 2005 Macroautophagy—a novel {beta}-amyloid peptide-generating pathway activated in Alzheimer's disease. J. Cell Biol. **171:** 87–98.

Communicating editor: K. G. Golic